

# Characterization of Polymer Synthesized from the Nonequilibrium Plasma Conversion of CFC-12 and Methane in a Dielectric Barrier Discharge Reactor

Sazal K. Kundu,<sup>†</sup> Eric M. Kennedy,<sup>\*,†</sup> John C. Mackie,<sup>†</sup> Clovia I. Holdsworth,<sup>§</sup> Thomas S. Molloy,<sup>†</sup> Vaibhav V. Gaikwad,<sup>†</sup> and Bogdan Z. Dlugogorski<sup>‡</sup>

<sup>†</sup>Process Safety and Environment Protection Research Group, School of Engineering and <sup>§</sup>Discipline of Chemistry, School of Environmental and Life Sciences, The University of Newcastle, Callaghan, New South Wales 2308, Australia

<sup>‡</sup>School of Engineering and Information Technology, Murdoch University, Murdoch, Western Australia 6150, Australia

**ABSTRACT:** A dielectric barrier discharge (DBD) nonequilibrium plasma reactor was employed to polymerize CFC-12 ( $\text{CCl}_2\text{F}_2$ , dichlorodifluoromethane) at atmospheric pressure. The plasma polymerization of this saturated halogenated hydrocarbon was conducted in the presence of methane as reactant, in an argon bath gas and where the reaction environment was free from oxygen and nitrogen. The reaction resulted in the formation of non-cross-linked polymer product and whereby the non-cross-linked nature of the polymer enabled its characterization by solution state  $^{13}\text{C}$  and  $^{19}\text{F}$  nuclear magnetic resonance (NMR) spectroscopic analysis. The generated polymer was also analyzed by Fourier transform infrared (FTIR) spectrometry, and the spectra thus obtained were consistent with the analysis by NMR. The analyses of NMR and FTIR spectroscopy reveal the formation of fluoropolymers from the conversion of CFC-12.

## 1. INTRODUCTION

The serious and detrimental effects of chlorofluorocarbons (CFCs) on the earth's ozone layer, and their contribution to global warming, have led to the end of manufacturing of these compounds, although significant quantities of these materials remain in service. Once a CFC has reached its end of use, proper disposal is then essential, and a significant body of research on the conversion of CFCs into environmentally benign substances has been reported.<sup>1,2</sup> Conventional thermal reactors (catalytic and noncatalytic) and, to a much lesser extent, plasma reactors have been employed for this purpose.

The application of a nonequilibrium plasma for treatment of CFCs has largely focused on the complete destruction of the target CFC.<sup>3–5</sup> Wallis et al., for example, studied the catalytic destruction of  $\text{CCl}_2\text{F}_2$  in nitrogen and in air using a dielectric pellet-bed plasma reactor,<sup>4</sup> while Wang et al. examined the decomposition of  $\text{CCl}_2\text{F}_2$  in an RF excited plasma reactor.<sup>5</sup>

Nonequilibrium plasmas have also been employed for the deposition of fluorocarbon polymer films, although the focus of these studies has been on perfluorocarbons (PFCs) and hydrofluorocarbons (HFCs) as feed materials, and the polymeric material thus formed is comprised primarily of cross-linked polymers. The application of these films include providing coatings or layers on devices (e.g., biopassivation coatings on implantable devices or interlayer dielectric films for integrated circuits).<sup>6</sup> Vinogradov et al. studied the deposition of polymer films in a DBD reactor operating at atmospheric pressure employing  $\text{CF}_4$ ,  $\text{C}_2\text{F}_6$ ,  $\text{C}_2\text{H}_2\text{F}_4$ ,  $\text{C}_3\text{F}_8$ ,  $\text{C}_3\text{HF}_7$ , and  $\text{C}_4\text{F}_8$  as feed,<sup>7,8</sup> while Wei et al. worked with  $\text{C}_4\text{F}_8$  and reported the formation of cross-linked polymer films in a DBD reactor operating at relatively low pressures (25–125 Pa).<sup>6</sup> Additives like hydrogen or methane have been used in some studies, and in the synthesis of polymer films from hexafluoropropene

( $\text{C}_3\text{F}_6$ ), Mountsier et al. employed hydrogen as an additive,<sup>9</sup> while Ingaki et al. studied the effect of methane as an additive.<sup>10</sup>

Plasma polymerization is a distinctly different process to conventional polymerization. The chemistry of plasma polymerization is generally much more complex than conventional polymerization due to the diversity of reactive species present,<sup>11</sup> and this complex chemistry gives rise to the opportunity to polymerize unconventional starting materials such as saturated alkanes or aromatics.<sup>12,13</sup>

While CFC-12 and methane are saturated compounds, the reactive species, formed in plasma, are polymerizable, and the formation of non-cross-linked fluoropolymers was found in the present study. The formation of a non-cross-linked polymer is advantageous and beneficial from a research perspective as it enables the use of solution-state NMR techniques for characterization of the polymer and these analyses aid in the development of an improved understanding of plasma polymerization chemistry.

The present article discloses follow-up work to our recent publication,<sup>14</sup> where we discussed the conversion of  $\text{CCl}_2\text{F}_2$  under various reaction conditions in the treatment of  $\text{CCl}_2\text{F}_2$  with methane in a dielectric barrier discharge nonequilibrium plasma. The targeted products from the treatment of  $\text{CCl}_2\text{F}_2$  with methane are value-added polymeric materials, and the current article presents a detailed structural analysis of the synthesized polymers together with a discussion of their synthesis mechanism.

**Received:** June 25, 2014

**Revised:** November 20, 2014

**Accepted:** November 23, 2014

**Published:** November 24, 2014

## 2. EXPERIMENTAL SECTION

The dielectric barrier discharge reactor used for this investigation consists of two cylindrical concentric dielectric tubes (alumina, 99.8% purity) and has been described in detail elsewhere.<sup>15</sup> The outer dielectric dimensions are 23 mm OD and 2 mm wall thickness and the inner dielectric dimensions are 10 mm OD and 1 mm wall thickness. The entire reactor assembly is operated in a dedicated fume cupboard. The power supply employed for this study can deliver a sinusoidal waveform at up to 20 kV (rms) at a fixed frequency of 21.5 kHz. Experimental results were expressed in this article in terms of input energy density. The input energy density was controlled by a component of the power supply component known as variac which is, basically, a variable transformer. At a set variac voltage, a voltage-charge Lissajous figure needs to be constructed on cathode ray oscilloscope to estimate power input to the reactor, the value of which can be converted to input energy density ( $P/F$ , where  $P$  is the power input to the reactor and  $F$  is the total volumetric feed rate). The detailed procedure for calculating power input to the reactor can be found in our earlier publication,<sup>16</sup> with a slight modification as described in a later publication.<sup>14</sup>

The feed gases were argon (99.999%, Coregas), CFC-12 (99.98%, Actrol), and methane (99.95%, Linde), and the feed streams were controlled by mass flow controllers (Brooks). The results presented in this article were generated with a feed condition of 1.25%  $\text{CCl}_2\text{F}_2$  and 1.25%  $\text{CH}_4$  in argon at  $100 \text{ cm}^3 \text{ min}^{-1}$ . The residence time ( $L/(F/A)$ , where  $L$  is the length of the electrode,  $F$  is the total volumetric feed rate, and  $A$  is the annular cross sectional area bounded by the dielectrics) for all experiments was 2.95 s.

Each experiment was conducted for 90 min in duration, and, on termination of the experiment, the reactor system was purged with argon. The DBD reactor was then dismantled, and the reactor tubes were rinsed with tetrahydrofuran solvent (99.9%, Merck). The eluted solution contains a polymeric mixture, which was used for polymer characterization by various analytical techniques.

The polymer-tetrahydrofuran solution, collected by rinsing the reactor tubes, was dried in a fume cupboard. A polymeric sample of known concentration was prepared by dissolving a portion of the dried polymer in the tetrahydrofuran solvent. A gel permeation chromatograph (GPC) of Waters GPCV 2000 model was employed to analyze this polymeric sample and quantify the molecular weight of polymers. The GPC is equipped with a refractive index (RI) detector and three Styragel columns (HR5E, HR3, and HR0.5) operating at  $40^\circ\text{C}$ . For calibration, polystyrene standards (Polymer Standards Service) with a molecular weight range of 470 to 2,300,000  $\text{g mol}^{-1}$  ( $M_n$ ) were used, and, therefore, the reported values of molecular weights of polymers in this article are based on polystyrene standards.

The structural analyses of the polymers were conducted by FTIR and NMR spectroscopies. The Fourier transform infrared (FTIR) analysis of polymers was conducted by an ATR (attenuated total reflectance)-FTIR (PerkinElmer Spectrum 2), while NMR experiments were conducted in a Bruker Avance 400 MHz spectrometer. A portion of the dried polymeric material was introduced directly into this FTIR for analysis.

In order to undertake NMR analyses, polymeric mixtures from four sets of experiments (operating under identical

conditions) were accumulated. A concentrated solution was prepared by dissolving the dried polymeric material in tetrahydrofuran solvent, whereupon the concentrated polymeric solution was transferred dropwise into a beaker of methanol (99.9%, Scharlau). Approximately one-third of the methanol solution was then removed from the top of the beaker, and the remainder was initially dried in the fume cupboard and then dried in a vacuum oven (operating at  $40^\circ\text{C}$ ). This procedure enhanced the concentration of high molecular weight fraction in the dried polymeric mixture. A detailed discussion of this procedure can be found elsewhere.<sup>17</sup> The dried polymeric samples were dissolved in deuterated chloroform (99.96 atom % D, 0.03% v/v TMS, Aldrich) solvent and used for NMR analyses. Bruker Topspin 3.1 was used for processing NMR spectra. The high molecular weight polymeric fraction enrichment procedure assists in obtaining NMR spectra that clearly highlight the features attributable to both high (broad peaks) and low (sharp peaks) molecular weight fractions.

## 3. RESULTS AND DISCUSSION

**3.1. Polymer Architecture.** The plasma polymerization of  $\text{CCl}_2\text{F}_2$  with methane in an argon bath gas was carried out over an input energy density range of 3–13  $\text{kJ L}^{-1}$ . The polymeric material thus synthesized readily dissolves in tetrahydrofuran and chloroform solvents. This observation in itself indicates that the polymer is mainly non-cross-linked but may be branched. The stability of polymer solutions in tetrahydrofuran and chloroform solvents was visually assessed over a period of several months with no observable precipitation or solid deposition. The non-cross-linked nature of the polymers provides several advantages, including the fact that they can be reshaped as required by heating. In addition, being fluorinated polymers, these materials have improved temperature stability, and they are resistant to most corrosive chemicals as compared to many nonfluorinated polymers. At the highest value of input energy density (13  $\text{kJ L}^{-1}$ ) investigated, trace quantities of the polymeric products were insoluble in tetrahydrofuran and chloroform solvents, indicating that some cross-linked polymer had formed under these conditions. The polymer characterization in this article is therefore primarily focused on the non-cross-linked portion of the polymer synthesized.

**3.2. Molecular Weight Distribution of Polymers.** According to GPC analysis, the polymeric material is comprised of two fractions—the number-average molecular weight ( $M_n$ ) of the low molecular weight fraction is  $550 \text{ g mol}^{-1}$  with a polydispersity index (PDI) of 1.2, while the  $M_n$  value of high molecular weight fraction is  $4600 \text{ g mol}^{-1}$  with a PDI value of 1.4. The values of polymer molecular weight and molecular weight distribution presented are of the polymers synthesized at 9  $\text{kJ L}^{-1}$ . Variation of  $M_n$  values with input energy density is minimal over the investigated range of input energy densities between 3–13  $\text{kJ L}^{-1}$ ; as an example, the  $M_n$  value of low and high molecular weight fractions are  $540 \text{ g mol}^{-1}$  and  $4200 \text{ g mol}^{-1}$ , respectively, at 5  $\text{kJ L}^{-1}$ . The  $M_n$  value of the high molecular weight polymer fraction, presented in our earlier study,<sup>15</sup> is somewhat different than the results obtained in the present study. This is because the analysis in the earlier publication was affected by the filter material used for the preparation of samples for GPC. While GPC is a precise and reliable method for quantifying molecular weight of polymers,<sup>18</sup> the filtration of samples is important as a highly aggressive

solvent, THF, is involved in the analysis. The filtration problem which occurred earlier was eliminated in the present study, and, therefore, a corrected value of molecular weight for the high molecular weight fraction was measured.

### 3.3. Characterization of Polymers by FTIR Spectrum.

Figure 1 presents a typical FTIR spectrum of polymers,

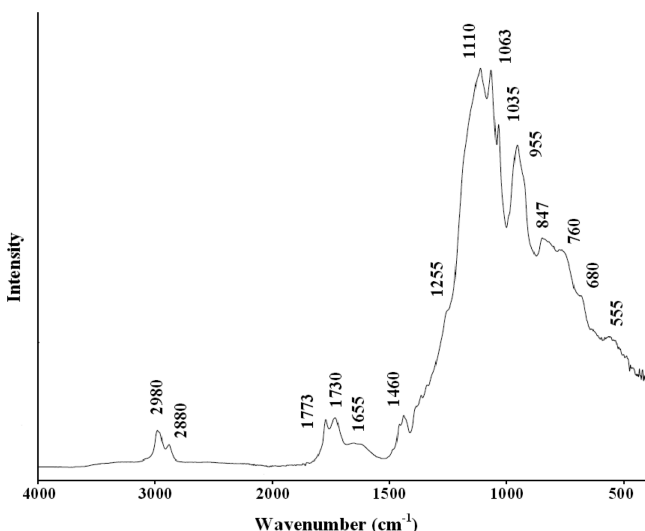


**Figure 1.** FTIR spectrum for the polymer synthesized at  $9 \text{ kJ L}^{-1}$  from the nonequilibrium plasma reactions between  $\text{CCl}_2\text{F}_2$  and  $\text{CH}_4$ .

synthesized at an energy density of  $9 \text{ kJ L}^{-1}$ . A  $\text{CF}_2$  bending vibration is present at the wavenumber of  $555 \text{ cm}^{-1}$  in the spectrum,<sup>19</sup> while the signals at  $680$  and  $955 \text{ cm}^{-1}$  arise from C–Cl stretching modes of various C–Cl functional groups (such as  $\text{CHCl}$  or  $\text{CHClF}$ ).<sup>20,21</sup> The absorption band at  $760 \text{ cm}^{-1}$  is likely to be associated with a  $\text{CH}_2$  rocking vibration, while the peak at  $847 \text{ cm}^{-1}$  may be assigned to either a  $\text{CH}_2$  or  $\text{CF}_2$  rocking vibration.<sup>22,23</sup> The signals at  $1035$ ,  $1063$ ,  $1110$ , and  $1255 \text{ cm}^{-1}$  are assigned to the C–F stretching modes of various functional groups (for example  $\text{CHF}$ ,  $\text{CHClF}$ ,  $\text{CHF}_2$ ,  $\text{F–C=CF}$ ,  $\text{CF}_2$ , and  $\text{CF}_3$ ).<sup>19,24,25</sup> The absorption band at  $1460 \text{ cm}^{-1}$  can be assigned to either a  $\text{CH}_3$  asymmetric bending or a  $\text{CH}_2$  scissoring vibration.<sup>22</sup> The signals at  $1773$  and  $1730 \text{ cm}^{-1}$  may be assigned to the internal double bonds of  $\text{FC=CF}_2$  and  $\text{FC=CF}$ ,<sup>26</sup> while the peak at  $1655 \text{ cm}^{-1}$  is most likely due to C=C stretching of the double bonds of  $\text{HC=CF}$ . The absorption bands at  $2880$  and  $2980 \text{ cm}^{-1}$  represent  $\text{CH}_3$  asymmetric and symmetric stretching vibrations.<sup>22</sup> The presence of various functional groups in the polymer chain identified by FTIR analysis is also established by the spectral signatures of various NMR experiments presented in the following section. The following section also discusses the analyses of various NMR spectra as well as the structure of the synthesized polymers.

**3.4. Structural Analysis of Polymers by NMR Experiments.** A series of solution state NMR experiments including  $^{13}\text{C}$  and  $^{19}\text{F}$  were conducted to characterize the structure of the polymer, and these analyses were enhanced by the use of two additional NMR techniques – DEPT 135 (Distortionless Enhancement by Polarization Transfer at  $135^\circ$  angle) and DEPTQ 135 (Distortionless Enhancement by Polarization Transfer at  $135^\circ$  angle, including the detection of quaternary nuclei).<sup>27</sup> The DEPT 135 experiments were used to distinguish  $\text{CH}_3$  and  $\text{CH}$  from  $\text{CH}_2$  moieties. In a complementary fashion,

the DEPTQ 135 experiments were used to distinguish signals of  $\text{CH}_3$  and  $\text{CH}$  groups from  $\text{CH}_2$  and quaternary carbons signals (groups that do not have any hydrogen atom; e.g.,  $\text{CF}_2$ ,  $\text{CF}_3$  etc.).<sup>28,29</sup> Based on a comparison of DEPTQ 135 and DEPT 135 spectra, it is possible to distinguish quaternary carbon species present in the polymer. The NMR analyses presented here are focused on the high molecular weight fractions, and the groups present in this fraction are characterized by the broad shaped peaks in the NMR spectra. In addition to these broad absorbances, there are also sharp peaks that are representative of the absorbances from the functional groups of the low molecular weight polymeric fractions.

The  $^{13}\text{C}$  NMR spectra disclose chemical shifts that can be attributed to several functional groups present in the polymers (Figure 2). The  $^{13}\text{C}$  absorbances at chemical shifts of 20, 44, 53,

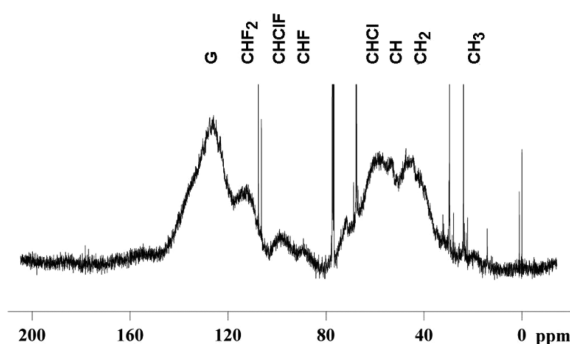


**Figure 2.**  $^{13}\text{C}$  NMR spectrum for the polymeric mixture synthesized at  $9 \text{ kJ L}^{-1}$  from the nonequilibrium plasma reactions between  $\text{CCl}_2\text{F}_2$  and  $\text{CH}_4$  (G indicates  $\text{CF}_2$ ,  $\text{CF}_3$  as well as  $\text{CH}$ ,  $\text{CF}$  and  $\text{CF}_2$  groups with double bonds).

58, 89, 99, and 112 ppm represent signals from  $\text{CH}_3$ ,  $\text{CH}_2$ ,  $\text{CH}$ ,  $\text{CHCl}$ ,  $\text{CHF}$ ,  $\text{CHClF}$ , and  $\text{CHF}_2$  groups, respectively. As disclosed by FTIR analysis, the polymer product contains species which are comprised of double bonds, including  $\text{HC=CF}$ ,  $\text{FC=CF}$ , and  $\text{FC=CF}_2$ . An additional double bond is present as  $\text{HC=CH}$ , from which the signal is very weak in the FTIR spectrum (at  $3082 \text{ cm}^{-1}$ ). The groups with double bonds ( $\text{HC=CH}$ ,  $\text{HC=CF}$ ,  $\text{FC=CF}$ , and  $\text{FC=CF}_2$ ) along with  $\text{CF}_2$  and  $\text{CF}_3$  groups show overlapping signals at 126 ppm in the  $^{13}\text{C}$  NMR spectrum. The DEPTQ 135 (Figure 3) spectrum

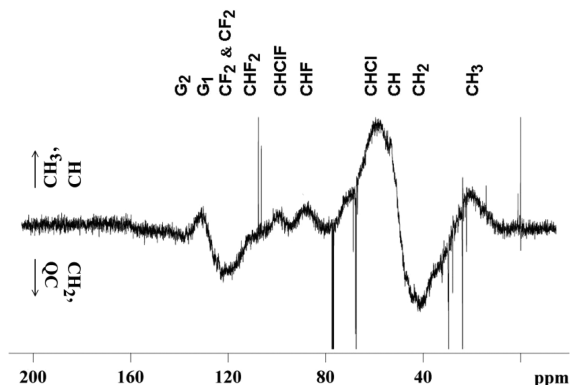


**Figure 3.** DEPTQ 135 NMR spectrum for the polymeric mixture synthesized at  $9 \text{ kJ L}^{-1}$  from the nonequilibrium plasma reactions between  $\text{CCl}_2\text{F}_2$  and  $\text{CH}_4$  ( $G_1$  indicates  $\text{CH}$  groups with double bonds and  $G_2$  indicates  $\text{CF}$  and  $\text{CF}_2$  groups with double bonds).



resolves the peak into two separate absorbances—one of them highlighting a quaternary carbon peak (which includes  $\text{CF}_2$  and  $\text{CF}_3$  groups) at 120 ppm, while another represents CH groups (from  $\text{HC}=\text{CH}$  and  $\text{HC}=\text{CF}$  groups) at 130 ppm. There is also a weak signal at 140 ppm in the DEPTQ 135 spectrum, which shows signals from CF and  $\text{CF}_2$  groups (from  $\text{HC}=\text{CF}$ ,  $\text{FC}=\text{CF}$ , and  $\text{FC}=\text{CF}_2$  groups). The DEPT 135 spectrum (Figure 4) shows a peak at 130 ppm, and peaks at either 120 or

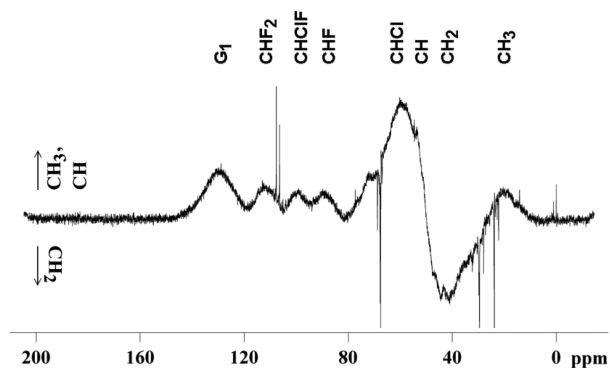


**Figure 4.** DEPT 135 NMR spectrum for the polymeric mixture synthesized at  $9 \text{ kJ L}^{-1}$  from the nonequilibrium plasma reactions between  $\text{CCl}_2\text{F}_2$  and  $\text{CH}_4$  ( $G_1$  indicates CH groups with double bonds).

140 ppm are absent. Therefore, it can be concluded that the groups exhibiting 120 and 140 ppm peaks result from quaternary carbon groups.

The  $^{19}\text{F}$  NMR spectrum of the polymer (Figure 5) discloses absorbances at  $\sim 50$  to  $\sim 90$ ,  $\sim 90$  to  $\sim 150$ , and  $\sim 150$  to  $\sim 210$

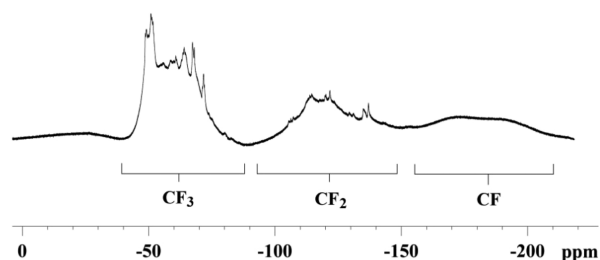


**Figure 5.**  $^{19}\text{F}$  NMR spectrum for the polymeric mixture synthesized at  $9 \text{ kJ L}^{-1}$  from the nonequilibrium plasma reactions between  $\text{CCl}_2\text{F}_2$  and  $\text{CH}_4$ .

ppm in the  $^{19}\text{F}$  NMR spectrum, representing signals from  $\text{CF}_3$ ,  $\text{CF}_2$ , and CF peaks, respectively. The CF peak in the  $^{19}\text{F}$  NMR spectra arises from CHF and  $\text{CHClF}$  groups and the CF of the double bond containing groups (such as  $\text{HC}=\text{CF}$ ,  $\text{FC}=\text{CF}$ , and  $\text{FC}=\text{CF}_2$ ). The  $\text{CF}_2$  peak in the  $^{19}\text{F}$  NMR spectrum stems from a bifunctional  $\text{CF}_2$  group, a  $\text{CHF}_2$  group, and  $\text{CF}_2$  from  $\text{FC}=\text{CF}_2$ . These spectral assignments have been made with the assistance of published references.<sup>30,31</sup>

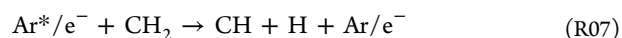
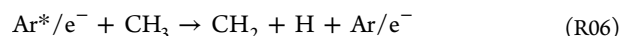
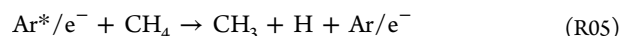
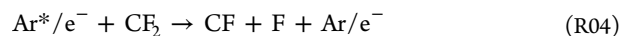
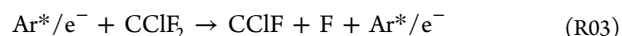
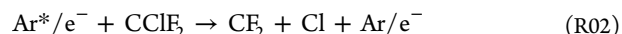
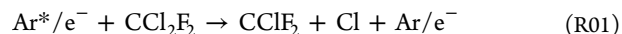
According to the NMR and FTIR spectral analyses, it can be concluded that the synthesized polymers are random copolymers where  $\text{CH}_2$ ,  $\text{CHCl}$ ,  $\text{CHF}$ ,  $\text{CF}_2$ ,  $\text{HC}=\text{CH}$ ,  $\text{HC}=\text{CF}$ , and  $\text{FC}=\text{CF}$  are all present in the backbone of the polymer chain. The CH peak at a chemical shift of 53 ppm of  $^{13}\text{C}$  NMR spectrum is also present in the backbone of the polymer chain including  $\text{CH}_3$ ,  $\text{CHF}_2$ ,  $\text{CHClF}$ ,  $\text{FC}=\text{CF}_2$ , and  $\text{CF}_3$  groups. The low molecular weight fraction polymers may also have all or some of the groups identified in the high

molecular weight fraction polymer; however, they are also random copolymers with relatively short chain lengths.

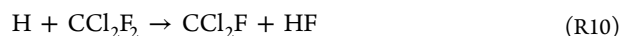
**3.5. Polymerization Mechanism.** In order to understand the complex chemistry of plasma polymerization, we have previously developed a polymerization mechanism based on the reaction of HFC-134a ( $\text{CF}_3\text{CH}_2\text{F}$ ) in an argon bath gas.<sup>17</sup> In the present article, two reactants were employed instead of a single reactant, and, therefore, the plasma chemistry includes a number of additional reactive species. The analyses by NMR, FTIR, and GPC show qualitative agreement with the mechanism proposed earlier for HFC-134a polymerization.

The reaction of  $\text{CCl}_2\text{F}_2$  and  $\text{CH}_4$  in an argon bath gas in the nonequilibrium plasma environment of a dielectric barrier discharge reactor generates gas phase species as well as polymeric products. The mechanism in the formation of gaseous species has been described in detail in our earlier publication.<sup>14</sup> In this article, mechanistic discussions in the formation of various radicals in the plasma reactor as well as their reaction in the synthesis of polymers are presented.

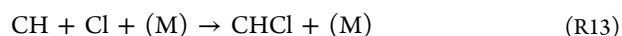
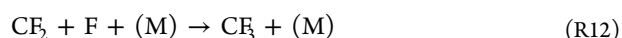
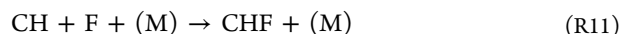
Reactant molecules decompose and form radicals via collisions with kinetic plasma electrons as well as with metastable state argon atoms. A significant quantity of metastable state argon atoms are formed in this system due to the presence of abundant argon atoms where their formation occurs through collisions of neutral argon atoms with fast electrons or through the radiative recombination of argon ions with slow electrons.<sup>32–34</sup> Representative reactions for the decompositions of  $\text{CCl}_2\text{F}_2$  and  $\text{CH}_4$  in the formation of various radicals are given below:<sup>15</sup>

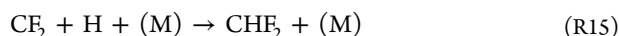


The radicals (including  $\text{CH}_2$ ,  $\text{CH}_3$ ,  $\text{CF}_2$ ) can participate in recombination and abstraction reactions. While a variety of gaseous product species (e.g.,  $\text{H}_2$ ,  $\text{HCl}$ ,  $\text{HF}$ )<sup>2,35–37</sup> are produced from these reactions, these processes also lead to the formation of various radicals. Some examples of these reactions are given below:



Radicals can also react to form different radical species. The formation of  $\text{CHF}$ ,  $\text{CF}_3$ ,  $\text{CHCl}$ ,  $\text{CHClF}$ , and  $\text{CHF}_2$  radicals may be explained by the following reactions:<sup>14</sup>





Many researchers have undertaken studies in order to unravel the complex mechanisms involved during plasma polymerization.<sup>38–40</sup> Denaro et al., for instance, proposed a radical-based mechanism, where radicals, generated in plasma, are trapped in polymer films and subsequently undergo polymerization.<sup>41</sup> Yasuda et al. proposed an alternative scheme, an atomic polymerization mechanism, where monomers become fragmented, and active species are subsequently formed, deposit, and polymerize.<sup>42</sup> In contrast to radical and atomic mechanisms, Westwood proposed a cationic or positive ions based plasma polymerization mechanism.<sup>43</sup> While studying plasma polymerization of several vinyl monomers, Westwood observed that the deposition of polymers took place only on the cathode (negatively charged electrode) in a DC discharge, whereas deposition of polymers was found on both electrodes in an AC discharge. Based on these findings, Westwood suggested that positive ions (cations) play a dominant role in plasma polymerization. The observed polymerization of the vinyl monomers, which deposits almost exclusively on the cathode with a DC discharge in Westwood's experiments, cannot be explained by radical<sup>41</sup> and atomic<sup>42</sup> polymerization mechanisms. While Westwood's mechanism seems consistent with plasma polymerization, as plasma is an ionization phenomena and the Coulombic effect cannot be ignored, a detailed explanation is needed to explain a major finding of the present investigation, most notably where non-cross-linked polymers of different molecular weight ranges were observed. The mechanistic discussion presented below is therefore based on Westwood's cationic mechanism with additional explanation on the formation of non-cross-linked polymers of different molecular weight ranges.

Cations are formed via direct electron impact reactions. Some examples of direct electron impact ionization reactions are given below:



The lowest energy metastable argon atoms (11.55 eV<sup>44</sup>) can ionize many species present in the plasma (for example  $\text{CH}_3$ –9.80 eV,<sup>45</sup>  $\text{CF}_3$ –9.25 eV<sup>46</sup>). This process is known as Penning ionization. Some examples of Penning ionization reactions for this system are given below:

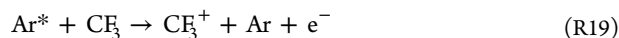
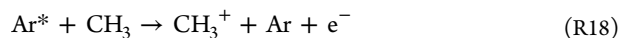
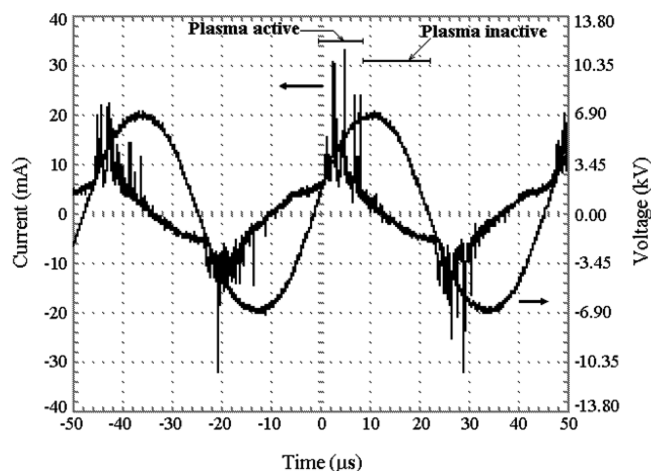


Figure 6 shows a typical instantaneous current and voltage waveform as generated in the present study, where each half AC cycle can be divided into a plasma active period and a period where electrical excitation is absent. As can be seen in Figure 6, the duration of electrical excitation in the system is 8–12  $\mu\text{s}$  in a 23  $\mu\text{s}$  half AC cycle, while the lifetime of metastable argon can be as long as 1.3 s.<sup>47</sup> As the lifetime of the radicals and metastable argon atoms are longer than the periods of no electrical excitation, the reactions R18 and R19 may occur continuously despite periodic excitation.

In a given AC half cycle, charged species in the plasma system experience Coulombic forces due to the electric field resulting from the applied voltage. As the electric field direction is radial in the concentric electrode geometry, cations formed in



**Figure 6.** Instantaneous current and applied voltage trace at 9 kJ L<sup>-1</sup> for the reaction of 1.25%  $\text{CCl}_2\text{F}_2$  and 1.25%  $\text{CH}_4$  in argon at 100 cm<sup>3</sup> min<sup>-1</sup> feed rate.

the discharge will drift toward the dielectric covering the momentary cathode while negatively charged species, mainly electrons, will drift toward the dielectric covering the momentary anode. On the subsequent AC half cycle, reversal of the electric field direction results in a reversal in the direction of the drift. It is presumed that drift in charged species leads to the development of transient regions of increased species concentration in the regions close to the dielectrics and may account for the observed cathodic deposition reported by Westwood in DC experiments.<sup>43</sup>

Based on GPC and NMR analyses, the polymeric materials contain a low molecular weight fraction as well as a high molecular weight fraction. The low molecular weight fraction is most likely the primary polymeric products. According to NMR analyses, the polymers contain many functional groups, and combining Westwood's observation as well as the NMR analyses, the chain propagation of low molecular weight polymers may be explained as



where  $\text{A}^+$  represents a cation (e.g.,  $\text{CH}_3^+$ ,  $\text{CF}_3^+$  etc.) that initiates the polymerization process and  $\text{B}\cdot$  or  $\text{C}\cdot$  represents a biradical (e.g.,  $\text{CF}_2$ ,  $\text{CHCl}$ ,  $\text{CHCF}_3$ , etc.) that reacts and propagates the polymeric chain. Previously, a cation-radical transformation polymerization mechanism was proposed for a conventional polymeric system.<sup>48</sup> The polymer chain may terminate by charge neutralization processes via an addition of a slow electron.

A portion of the low molecular weight fraction is most likely subsequently converted to high molecular weight fraction via successive plasma activity. Radicals are formed on the structure of the polymeric species via continual impact of kinetic plasma electrons.<sup>49,50</sup> The linkage reactions at radical sites within low molecular weight polymers then form the high molecular weight polymers. The difference between low and high molecular weight polymers indicates that this linkage occurs within several low molecular weight polymer molecules. In this way, high molecular weight polymer molecules are synthesized from the reactivation and subsequent linkage of low molecular weight polymer molecules. Therefore, the groups present in the low molecular weight fraction polymers are also present in the

high molecular weight fraction, as described in the polymer characterization section.

As described in polymer architecture section, a trace amount of cross-linked polymers are formed at  $13 \text{ kJ L}^{-1}$ . When kinetic plasma electrons generate radical sites on non-crosslinked polymers, cross-linking reactions may occur at radical sites among non-cross-linked polymers which lead to the formation of crosslinked polymers.

#### 4. CONCLUSION

Plasma polymerization of  $\text{CCl}_2\text{F}_2$  was studied in a dielectric barrier discharge nonequilibrium plasma reactor, where methane was employed as a reactant and in which oxygen and nitrogen were excluded from the feed. According to the experimental findings, the synthesized polymers are mainly non-cross-linked fluoropolymers. Structural analyses of the polymers by FTIR and NMR spectroscopy reveal that the polymers are random copolymers and consist of functional groups including  $\text{CH}_3$ ,  $\text{CH}_2$ ,  $\text{CHCl}$ ,  $\text{CHF}$ ,  $\text{CF}_2$ ,  $\text{CHF}_2$ ,  $\text{CHClF}$ , and  $\text{CF}_3$ . The synthesis mechanism of two different molecular weight range polymers, identified by GPC and NMR, was discussed, based on plasma phenomena as well as structural analyses by FTIR and NMR spectroscopy. The synthesis of non-cross-linked fluoropolymers can be a potential pathway to treat waste CFC-12, by transposing it into a material which may have commercial value.

#### AUTHOR INFORMATION

##### Corresponding Author

\*E-mail: eric.kennedy@newcastle.edu.au.

##### Notes

The authors declare no competing financial interest.

#### ACKNOWLEDGMENTS

The authors would like to thank the Australian Research Council for financial support of this project. Szal K. Kundu and Vaibhav V. Gaikwad are indebted to the Australian Government and the University of Newcastle, Australia for postgraduate scholarships. We thank Dr. Monica Rossignoli and Ms. Azrinawati Mohd Zin at School of Environmental and Life Sciences, The University of Newcastle, Australia for their assistance with NMR and GPC analyses.

#### REFERENCES

- (1) Yu, H.; Kennedy, E. M.; Adesina, A. A.; Dlugogorski, B. Z. A review of CFC and halon treatment technologies - The nature and role of catalysts. *Catal. Surv. Asia* **2006**, *10* (1), 40–54.
- (2) Uddin, M. A.; Kennedy, E. M.; Dlugogorski, B. Z. Gas-phase reaction of  $\text{CCl}_2\text{F}_2$  (CFC-12) with methane. *Chemosphere* **2003**, *53* (9), 1189–1191.
- (3) Ricketts, C. L.; Wallis, A. E.; Whitehead, J. C.; Zhang, K. A mechanism for the destruction of CFC-12 in a nonthermal, atmospheric pressure plasma. *J. Phys. Chem. A* **2004**, *108* (40), 8341–8345.
- (4) Wallis, A. E.; Whitehead, J. C.; Zhang, K. Plasma-assisted catalysis for the destruction of CFC-12 in atmospheric pressure gas streams using  $\text{TiO}_2$ . *Catal. Lett.* **2007**, *113* (1), 29–33.
- (5) Wang, Y. F.; Lee, W. J.; Chen, C. Y. CFC-12 Decomposition in a RF plasma system. *J. Aerosol Sci.* **1997**, *28* (1001), 279–280.
- (6) Wei, L.; Xiaodong, T.; Dongping, L.; Yanhong, L.; Zhiqing, F.; Baoxiang, C. Growth of Fluorocarbon Films by Low-Pressure Dielectric Barrier Discharge. *Plasma Sci. Technol.* **2008**, *10* (1), 74–77.
- (7) Vinogradov, I. P.; Lunk, A. Structure and chemical composition of polymer films deposited in a dielectric barrier discharge (DBD) in

Ar/fluorocarbon mixtures. *Surf. Coat. Technol.* **2005**, *200* (1), 660–663.

- (8) Vinogradov, I. P.; Lunk, A. Dependence of surface tension and deposition rate of fluorocarbon polymer films on plasma parameters in a dielectric barrier discharge (DBD). *Surf. Coat. Technol.* **2005**, *200* (1), 695–699.

- (9) Mountsier, T. W.; Kumar, D. In *Fluorocarbon Films From Plasma Polymerization of Hexafluoropropylene and Hydrogen*; Materials Research Society Symposium Proceedings, 1997; Cambridge Univ Press: 1997; pp 41–46.

- (10) Inagaki, N.; Ohkubo, J. Plasma polymerization of hexafluoropropene/methane mixtures and composite membranes for gas separations. *J. Membr. Sci.* **1986**, *27* (1), 63–75.

- (11) Lau, K. K. S. Chemical vapor deposition of fluorocarbon films for low dielectric constant thin film applications. Ph.D. Thesis, Massachusetts Institute of Technology, 2000.

- (12) Shi, F. F. Recent advances in polymer thin films prepared by plasma polymerization synthesis, structural characterization, properties and applications. *Surf. Coat. Technol.* **1996**, *82* (1), 1–15.

- (13) Jiang, H.; Hong, L.; Venkatasubramanian, N.; Grant, J. T.; Eyink, K.; Wiacek, K.; Fries-Carr, S.; Enlow, J.; Bunning, T. J. The relationship between chemical structure and dielectric properties of plasma-enhanced chemical vapor deposited polymer thin films. *Thin Solid Films* **2007**, *515* (7), 3513–3520.

- (14) Kundu, S. K.; Kennedy, E. M.; Mackie, J. C.; Holdsworth, C. I.; Molloy, T. S.; Gaikwad, V. V.; Dlugogorski, B. Z. Study on the Reaction of  $\text{CCl}_2\text{F}_2$  with  $\text{CH}_4$  in a Dielectric Barrier Discharge Nonequilibrium Plasma. *Plasma Processes Polym.* **2013**, *10*, 912–921.

- (15) Kennedy, E. M.; Kundu, S. K.; Mackie, J. C.; Holdsworth, C. I.; Molloy, T. S.; Gaikwad, V. V.; Dlugogorski, B. Z. Conversion of fluorine-containing ozone-depleting and greenhouse gases to valuable polymers in a non-thermal plasma. *Ind. Eng. Chem. Res.* **2012**, *51* (34), 11279–11283.

- (16) Kundu, S. K.; Kennedy, E. M.; Gaikwad, V. V.; Molloy, T. S.; Dlugogorski, B. Z. Experimental investigation of alumina and quartz as dielectrics for a cylindrical double dielectric barrier discharge reactor in argon diluted methane plasma. *Chem. Eng. J.* **2012**, *180* (0), 178–189.

- (17) Kundu, S. K.; Kennedy, E. M.; Mackie, J. C.; Holdsworth, C. I.; Molloy, T. S.; Gaikwad, V. V.; Dlugogorski, B. Z. Non-equilibrium plasma polymerization of HFC-134a in a dielectric barrier discharge reactor; polymer characterization and a proposed mechanism for polymer formation. *IEEE Trans. Plasma Sci.* **2014**, *42* (10), 3095–3100.

- (18) *Solutions for molar mass determination*. Polymer Standards Service Web site. <http://www.polymer.de/solutions/molar-mass-determination/> (accessed Apr 17, 2014).

- (19) Bormashenko, Y.; Pogreb, R.; Stanevsky, O.; Bormashenko, E. Vibrational spectrum of PVDF and its interpretation. *Polym. Test.* **2004**, *23* (7), 791–796.

- (20) Lin, J.-C.; Tjong, S.-L.; Chen, C.-Y. Surface characterization and platelet adhesion studies on fluorocarbons prepared by plasma-induced graft polymerization. *J. Biomater. Sci., Polym. Ed.* **2000**, *11* (7), 701–714.

- (21) Simpson, D.; Plyler, E. K. Infrared spectra of pentachlorofluoroethane, 1,2-dichlorotetrafluoroethane, and 1-bromo-2-fluoroethane. *J. Res. Natl. Bur. Stand.* **1953**, *50* (5), 223–227.

- (22) Smith, B. C. *Infrared spectral interpretation: a systematic approach*; CRC Press: 1999.

- (23) Lanceros-Mendez, S.; Mano, J. F.; Costa, A. M.; Schmidt, V. H. FTIR and DSC studies of mechanically deformed  $\beta$ -PVDF films. *J. Macromol. Sci., Part B: Phys.* **2001**, *40* (3–4), 517–527.

- (24) Ji, Y.; Liu, J.; Jiang, Y.; Liu, Y. Analysis of Raman and infrared spectra of poly (vinylidene fluoride) irradiated by KrF excimer laser. *Spectrochim. Acta, Part A* **2008**, *70* (2), 297–300.

- (25) Mihály, J.; Sterkel, S.; Ortner, H. M.; Kocsis, L.; Hajba, L.; Furdyga, É.; Mink, J. FTIR and FT-Raman spectroscopic study on polymer based high pressure digestion vessels. *Croat. Chem. Acta* **2006**, *79* (3), 497–501.

- (26) Simons, J. H. *Fluorine chemistry*; Elsevier: 1954; Vol. 2, p 457.



- (27) Elipse, M. V. S. *LC-NMR and Other Hyphenated NMR Techniques: Overview and Applications*; John Wiley and Sons: Hoboken, New Jersey, 2012.
- (28) Burger, R.; Bigler, P. DEPTQ: distortionless enhancement by polarization transfer including the detection of quaternary nuclei. *J. Magn. Reson.* **1998**, *135* (2), 529–534.
- (29) Özdoga, T.; Orbay, M. A Theoretical Investigation of DEPTQ NMR Spectroscopy for I n S Spin System ( $I = 1/2$ ,  $S = 1/2$ ). *Spectrosc. Lett.* **2002**, *35* (3), 447–454.
- (30) Brandolini, A. J.; Hills, D. D. *NMR Spectra of Polymers and Polymer Additives*; Marcel Dekker: New York, 2000.
- (31) Foris, A.  $^{13}\text{C}$  NMR spectra of halocarbons. *Magn. Reson. Chem.* **2001**, *39* (7), 386–398.
- (32) Zhao, G.; Argyle, M. D.; Radosz, M. Optical emission study of nonthermal plasma confirms reaction mechanisms involving neutral rather than charged species. *J. Appl. Phys.* **2007**, *101* (3), 033303.
- (33) Skrzypkowski, M. P.; Johnsen, R.; Rosati, R. E.; Golde, M. F. Flowing-afterglow measurements of collisional radiative recombination of argon ions. *Chem. Phys.* **2004**, *296* (1), 23–27.
- (34) Sukhinin, G. I.; Fedoseev, A. V.; Khmel', S. Y. Role of secondary electrons and metastable atoms in the electron-beam activation of argon-silane mixtures. *Plasma Phys. Rep.* **2008**, *34* (1), 60–70.
- (35) Jones, W. E.; Skolnik, E. G. Reactions of fluorine atoms. *Chem. Rev.* **1976**, *76* (5), 563–592.
- (36) Simpson, W. R.; Rakitzis, T. P.; Kandel, S. A.; Lev-On, T.; Zare, R. N. Picturing the transition-state region and understanding vibrational enhancement for the  $\text{Cl} + \text{CH}_4 \rightarrow \text{HCl} + \text{CH}_3$  reaction. *J. Phys. Chem.* **1996**, *100* (19), 7938–7947.
- (37) Sutherland, J. W.; Su, M. C.; Michael, J. V. Rate constants for  $\text{H} + \text{CH}_4$ ,  $\text{CH}_3 + \text{H}_2$ , and  $\text{CH}_4$  dissociation at high temperature. *Int. J. Chem. Kinet.* **2001**, *33* (11), 669–684.
- (38) Hamerli, P. Plasma aminofunctionalisation of polymeric membrane surfaces for tissue engineering applications. Ph.D. Thesis, University of Veszprém, 2004.
- (39) Shen, M.; Bell, A. T. A review of recent advances in plasma polymerization. *ACS Symp. Ser.* **1979**, *108*, 1–33.
- (40) Friedrich, J. Mechanisms of Plasma Polymerization - Reviewed from a Chemical Point of View. *Plasma Process. Polym.* **2011**, *8* (9), 783–802.
- (41) Denaro, A. R.; Owens, P. A.; Crawshaw, A. Glow discharge polymerization - styrene. *Eur. Polym. J.* **1968**, *4* (1), 93–106.
- (42) Yasuda, H. K.; Yeh, Y. S.; Fusselman, S. A growth-mechanism for the vacuum deposition of polymeric materials. *Pure Appl. Chem.* **1990**, *62* (9), 1689–1698.
- (43) Westwood, A. R. Glow discharge polymerization-I. Rates and mechanisms of polymer formation. *Eur. Polym. J.* **1971**, *7* (4), 363–375.
- (44) Ferreira, C. M.; Loureiro, J.; Ricard, A. Populations in the metastable and the resonance levels of argon and stepwise ionization effects in a low pressure argon positive column. *J. Appl. Phys.* **1985**, *57* (1), 82–90.
- (45) *Handbook of Chemistry and Physics*; Lide, D. R., Ed.; CRC Press: Boca Raton, FL, 1991.
- (46) Lifshitz, C.; Chupka, W. A. Photoionization of the CF Free Radical. *J. Chem. Phys.* **1967**, *47*, 3439.
- (47) Van Dyck, R. S., Jr.; Johnson, C. E.; Shugart, H. A. Lifetime lower limits for the 3P0 and 3P2 metastable states of neon, argon, and krypton. *Phys. Rev. A* **1972**, *5* (2), 991.
- (48) Guo, H. Q.; Kajiura, A.; Morishima, Y.; Kamachi, M. Radical/Cation Transformation Polymerization and Its Application to the Preparation of Block Copolymers. *Polym. Adv. Technol.* **1997**, *8* (4), 196–202.
- (49) Cruz, G. J.; Morales, J.; Castillo-Ortega, M. M.; Olayo, R. Synthesis of polyaniline films by plasma polymerization. *Synth. Met.* **1997**, *88* (3), 213–218.
- (50) Wang, P.; Tan, K. L.; Kang, E. T.; Neoh, K. G. Plasma-induced immobilization of poly (ethylene glycol) onto poly (vinylidene fluoride) microporous membrane. *J. Membr. Sci.* **2002**, *195* (1), 103–114.